Celal Bayar University Journal of Science

Optimization and Mechanical Performance of Alkali-Activated Bottom Ash and Polypropylene Fiber in Deep Mixing Columns

Fatih Yılmaz[1], Büşra Avlayan[1], Hakan Alper Kamiloğlu[1]*

[1] Bayburt University, Enginnering Faculty, Civil Engineering Department, 6910, Bayburt Türkiye
* hkamiloglu@bayburt.edu.tr
* 0000-0003-3313-9239

Received: December 7, 2024
Accepted: July 1, 2025
DOI: 10.18466/cbayarfbe.1597869

Abstract

Deep mixing columns (DMC) are one of the widely used soil improvement methods in cohesive and cohesionless soils. Cement and lime are predominantly used as conventional binders in DMC grout. Due to high CO_2 emissions from conventional binders, the feasibility of using alkali-activated binders as DMC grout is being investigated. This study was conducted in three main stages. In the first stage, the proportions of bottom ash and activator (mixture of 10M NaOH and Na_2SiO_3) were optimized to achieve the highest UCS value using response surface methodology (RSM). In the second stage, the influence of polypropylene fiber content was examined in detail by incorporating varying amounts of fibers into the optimized binder-activator mixture to determine the optimal fiber content. Since DMC are fully buried, they are cured in the soil media. In this case, the soil temperature, which varies along the depth of the soil, also becomes the curing temperature of the DCM. Due to climate, soil condition and thermodynamic based parameters, curing temperature of the DMC varies throughout the soil depth. Therefore, in the third stage, the effect of curing temperature on the mechanical properties of the stabilized samples was evaluated under different temperatures. Results of the study revealed optimal UCS values with AAB content of 0.3-0.5 and activator content of 0.45-0.5. Polypropylene fiber reinforcement further improved strength, reaching an optimum at 1.50-1.75% content. Curing temperature played a significant role, with UCS and modulus of elasticity increasing up to 30 °C, indicating the importance of considering environmental factors in DMC design. These findings suggest that the optimized mixture has the potential to replace conventional cement-based binders in DMCs, offering a more sustainable solution with lower carbon emissions. Furthermore, the observed influence of curing temperature highlights the need to account for subsurface thermal variations when designing DMCs, as these factors significantly affect strength gain and long-term performance.

Keywords: Alkali activated binder, Curing temperature, Deep mixing column, Optimization, Polypropylene fiber

1. Introduction

Depending on the loads from the superstructure, the minimum engineering properties that the foundation soil should provide vary. Nowadays, the minimum engineering properties required by the superstructure cannot be met by the foundation soil. It is possible to attain desired soil qualities by using a variety of soil stabilizing techniques. Depending on the significant depth of the structure or the depth of the problematic soil, shallow or deep soil improvement methods can be used. Deep soil mixing (DSM) column, vibro compaction, stone column, dynamic compaction, and jet-grout injection are some of the widely used DSM. Compared to other deep stabilizing techniques, DSM offers a few benefits, such as reduced vibration, noise, and surface settlement [1]. Since the 1960s, DMC has been applied for soil stabilization. The technique is based on creating high-strength soil columns by mixing various kinds of binders and soil in soil media using an auger or cutter to mix soil and binder. The most commonly used conventional binders in deep mixing columns are cement and lime [2]. In DMC applications, the amount of binder needed for the columns range from 50 kg to 400 kg per cubic meter of soil [3]. Considering the number of deep mixing columns required for a project and the length of each column, which can be up to 30 m, it is seen that the amount of binder required for

deep mixing application is remarkable. Cement production is responsible for about 7 per cent of global CO_2 release [4]. The high carbon emission problem arising from the production process of conventional binders leads to the investigation of the use of alternative binders that are less harmful to the environment [5].

The last decades have seen an increase in research on the use of geopolymers and alkali-activated materials for soil stabilization applications. As an alternative to traditional binders, some research has concentrated on the availability of waste materials with low costs and minimal CO_2 emissions. Bottom ash, rice husk, ballast furnace slag, metakaolin, and volcanic tuff are some of the widely used agents that can be evaluated as alkali-activated binders for soil stabilization application [6]. Alkali activators play a vital role in creating alkali-alumina sources for geopolymer reactions, as they have a considerable effect on the dissolution of raw materials. $Ca(OH)_2$, LiOH, NaOH, Na_2CO_3, Na_2SiO_3, KOH, K_2CO_3, and K_2SiO_3 are widely used stabilization agents to activate binders in alkali-activated soil stabilization applications [7]. There are wide range of studies investigating the effects of several parameters on mechanical properties of stabilized soil with alkali activated additives. In wide range of studies the effects of binder type [8], alkali activator type [9], amount of additives [10] , molar ratios of basic oxides [11] on mechanical properties of the stabilized soil, and optimizing the additives were studied [12,13].

There is no doubt that determination of optimum ratios of basic oxides such as; SiO_2/Al_2O_3, Na_2SiO_3/NaOH, Na_2O/Al_2O_3, Na_2O/SiO_2, H_2O/ Na_2O, Si/Al, Na/Al, Si/Ca, or SiO_2/Na_2O has remarkable importance for geopolymer grouts [12, 14]. However, these molar ratios are not enough to evaluate the mechanical properties of soil due to neglecting moisture content, which is an important parameter for soil compaction in soil stabilization applications [15]. Therefore, activator and binder contents are required to be considered in the optimization of stabilization agents.

In addition to the increased mechanical properties, brittleness also increases in the improvement applications made with both traditional binders and alkali activated binders [16,17]. In order to overcome this negative phenomenon and to increase the ductility of the material, the use of fibers in stabilization applications is a common practice [18]. The addition of fibers DMC slurries prepared with alkali-activated binders appears to be a promising way to improve the mechanical properties and durability of these materials. The biggest problem in this regard is the ability of the fibers to pass through the nozzles in the DMC mixer without causing blockage. Despite concerns about the size limitations of the nozzles used in DMC applications, there are studies examining the usability of fibers in this type of application [19].

One of the major concerns for soil stabilization applications with alkali-activated material is to determine the optimum stabilization agent content. Several optimization techniques can be employed for the optimization of stabilizers. Response Surface Methodology (RSM), Taguchi approach, Artificial Inteligency are some of the methods which can be used for the optimization [20, 21]. RSM is a statistical and mathematical-based method that can be used for various purposes. RSM can be used for three purposes: (1) determining the ideal response value; (2) clearly examining the entire system; and (3) expediting complex numerical calculations [22]. Although it is not a new method in the literature, the use of RSM for optimization purposes in geotechnical applications is limited. Furthermore, very little research has been done on optimizing precursor and activator amounts by employing RSM for alkali-activated grout in deep mixed columns.

There are several studies on deep-mixing methods considering various aspects. The studies about the method can be summarized under three categories: experimental-numerical modeling, automation and monitoring, and use of alternative binders. Full scale or numerical models are employed to predict the bearing capacity [23], settlement [24], lateral load-bearing capacity [25], or lateral displacement [26] performance of the stabilized soil column. Additionally, employing deepmix columns to mitigate, slope failures and liquefaction, and dynamic response of the deepmix columns are investigating with numerical and experimental approaches [27]. There are several studies about advanced systems that automate mixing parameters and monitor mixing quality in real-time for improved control and efficiency. Automatic binder injection systems, computer-controlled mixing tools, real-time monitoring of mixing parameters, and non-destructive testing (NDT) techniques were studied within this context [3]. Investigating the usability of alternative binders for deep-mix columns is another issue that geotechnical engineers focused on. In this context, it is aimed to enhance the mechanical, durability, or seismic properties of mortars used for DMC [28]. Additionally, studies on investigating a new stabilizing agent or alternative binder to conventional binders receive widespread literature coverage [29].

DMC up to 30 m in length, which operate completely buried in the soil, take their cure from the soil environment in which they are formed. In this case, the soil temperature that changes throughout the soil depth is also the curing temperature of the deep mixing columns. The parameters such as annual mean air temperature, surface air temperature, and thermal conductivity of the soil play a vital role in the variation

of soil temperature along the soil depth [30]. Therefore, mostly the temperature along the soil depth differs significantly from the surface temperature. This causes the different curing temperatures of the deep mix columns along the soil depth. This affects the bearing capacity and settlement parameters of the columns. Although there is a wide range of studies about deepmixed columns, the studies investigating the effect of environmental temperature on the mechanical properties of the mortar of the DMC are very few.

Suggested study was novel in combining alkali-activated bottom ash with polypropylene fibers in deep mixing columns, optimized via RSM. It also uniquely investigates the effect of curing temperature under realistic subsurface conditions and includes a carbon footprint comparison, emphasizing both technical and environmental contributions. In context of the study, a mixture of a high plasticity clayey soil and alkali-activated bottom ash was prepared as a deep mixing column mortar. Within the scope of the study, it was aimed to 1) to optimize the deep mixing mortar components by response surface method, 2) to determine the effect of polypropylene fiber additive on the mechanical properties of the stabilized soil, 3) to determine the effect of curing temperature on the deep mixing column mortar prepared with alkali-activated bottom ash were aimed. This study was guided by the following hypotheses: (1) Alkali-activated bottom ash and optimized activator ratios can significantly improve the UCS of deep mixing column mortars; (2) The incorporation of polypropylene fiber improves ductility and further enhances mechanical performance up to an optimum dosage; (3) Curing temperature has a significant influence on the strength development of the geopolymer-stabilized soil, with higher temperatures promoting better mechanical properties. These hypotheses were tested through a systematic experimental design. In this context, soil samples of 50 mm diameter and 100 mm height were prepared considering the recommendations of Federal Highway Administration (FHWA) for deep mixing columns [30]. F-class bottom ash was used as the alkali-activated binder in the geopolymerization process. The mixture of 10 M NaOH solution and Na2SiO3 solutions was used as an alkali activator. The study comprises three stages. In the first stage, alkali-activated precursor and alkali activator amounts were optimized using Response Surface Methodology (RSM) to maximize UCS. In the second stage of the study, the UCS of the samples obtained by adding different amounts of 6 mm long polypropylene fiber reinforcement to the optimum amount of activator and binder were determined. Thus the reinforcement content that gives the maximum strength was obtained. In the third step of the study, soil samples were prepared considering optimum amounts of binder, activator, and reinforcement additives. The prepared samples were subjected to 5 °C, 10 °C, 20 °C, and 30 °C curing 5 °C, 10 °C, 20 °C, and 30 °C curing temperatures for 7 days and 28 days.

2. Materials

2.1. Soil

The soil used in the experiments was obtained from an observation well in Demirözü district of Bayburt province. The soil was classified as high plasticity clay (CH) according to ASTM D2487-17 standard. Some of the physical properties of the soil is presented in Table 1.

Table 1. Some of the physical properties of the soil

Physical properties	Value
Liquid limit	60.81%
Plastic limit	30%
Plasticity index	30.81%
Specific gravity	2.60
Optimum moisture content	22.5%
Maximum dry unit weight	16.30 kN/m^3
Soil class (USCS)	CH
Color	Xanthic

2.2. Bottom ash

Bottom ash (BA) comprising high calcium was used as a precursor in the study. The bottom ash used in this study was obtained from the Kangal coal-fired power plant, a government-regulated facility in Sivas/ Türkiye. Utilizing this industrial by-product in deep mixing columns not only diverts waste from landfills but also reduces dependency on high-carbon cementitious materials, supporting environmentally sustainable engineering practices. Oxide components of the precursor was determined with X-ray fluorescence (XRF) analyses and presented in Table 2. From the table it is seen that the bottom ash (FA) becomes prominent with CaO content.

Table 2. Oxide components of the bottom ash

Composition (%)	**CaO**	**Al_2O_3**	**Fe_2O_3**	**SiO_2**
	32.5	11.0	4.5	25.3
	MgO	**SO_3**	**Loss**	**Na_2O**
	3.70	3.6	7.05	0.4

2.3. Activator

To activate the bottom ash, a solution containing 10 M NaOH and Na_2SiO_3 was employed to create a high-alkali solution. H_2O (64.72%), SiO_2 (28.65%), Na_2O (8.85%) were the major components of the Na_2SiO_3 solution. The specific gravity of the solution was 1.46 g/cc. NaOH pellets with a purity of 98% were utilized to make a 10M NaOH solution. The activator used in the study was created by combining the prepared solutions at 50%-50% by mass.

2.4. Fiber

Polypropylene fiber with 6 mm length was used in soil stabilization applications. Corrosion resistance and alkali resistance of the fiber were high and tensile strength of the material was 600 MPa. Other mechanical properties of the fiber were presented in Table 3.

Table 3. Fiber properties used in the mixture

Properties	Value
Specific gravity	0.90 g/cm^3
Fiber length	6 mm
Elasticity modulus	3800 N/mm^2
Melting point	230

3. Sample preparation

The Federal Highway Administration (FHWA) design handbook for deep mixing columns was used to prepare the samples [31]. The alkali activator (50% NaOH–50% Na_2SiO_3) and bottom ash were pre-mixed for 3 minutes to ensure chemical activation. This slurry was then blended with the soil for 10 minutes using a Hobart planetary mixer at a constant speed of 140 rpm to achieve uniform distribution and consistency. High-fluidity slurries were gently tapped to release trapped air, while lower fluidity mixtures were compacted using a slender steel rod to avoid segregation. The slurries were put into 50 mm diameter sampling tubes. Using a thin rod, low consistency mixtures were crushed into a 50 mm diameter mold. High fluidity mixtures were put into the mold and tapped to liberate air pockets. The samples were prepared with a height of 100 mm in accordance with the FHWA's minimum height-to-diameter ratio requirements. The samples were covered in plastic film and cured at a constant temperature of 26ºC ±1 ºC. UCS values of the 7-day and 28-day cured samples were determined with UCS tests.

4. Statistical analyses with RSM approach

4.1. Experimental design

This part of the study, it was aimed to optimize the amount of precursor and activator to obtain maximum UCS using the response surface method (RSM). Design-Expert 12 statistical software was used for experimental design and statistical analyses. Central composite design (CCD) was used for α=0.5 in the experimental design. For this purpose, a five-level CCD was conducted to examine the effects of activator bottom ash (BA) amounts on the UCS value. In the experimental design, the weight percentages of the parameters were considered independent variables. These independent variables are X_1 = Bottom ash weight/soil weight, and X_2 = Activator weight/dry matter weight. The two independent variables were selected for the response surface analysis, bottom ash/soil ratio (X_1) and activator/dry matter ratio (X_2) were chosen based on their direct influence on the alkali activation process and UCS of the mixture. The bottom ash content governs the aluminosilicate availability, while the activator dosage controls the dissolution and polymerization reactions critical to strength development. These variables were also commonly optimized in similar stabilization studies, making them relevant for comparative assessment. The UCS of the specimens were considered as the response. The center points and upper and lower limits of the independent variables are presented in Table 4.

Table 4. The upper, lower, and central values of the independent variables

Independent Variables	Bottom ash/ soil X_1		Activator/dry matter X_2
	Coded	Actual	
Level of Factors	-1	0.1	0.25
	-0.5	0.2	0.337
	0	0.3	0.425
	+0.5	0.4	0.512
	+1	0.5	0.6

Cylindrical soil specimens were prepared considering the experimental design shown in Table 5. The design consists of 29 experiments. Within the scope of the experimental study, the amount of bottom ash and activator was determined according to Table 4 and mixed with the soil. The prepared mixtures were moulded according to the recommendations of FHWA. The specimens with 50 mm diameter and 100 mm height were cured for 7 days at constant temperatures of 5, 10, 20, and 30 ºC. The cured specimens were subjected to UCS tests in accordance with ASTM D2166. The UCS value obtained was evaluated as a response in the response surface design. The experimental design matrix and UCS values were presented in the table.

Table 5. Experimental design matrix

Runs	Actual		Response
	Bottom ash/soil X_1	Activator/dry matter X_2	UCS (MPa)
1	0.1	0.25	0.72
2	0.1	0.25	1.10
3	0.1	0.25	0.81
4	0.5	0.25	0.61
5	0.5	0.25	0.53
6	0.5	0.25	0.56
7	0.1	0.6	1.28
8	0.1	0.6	1.49
9	0.1	0.6	1.28
10	0.5	0.6	2.10
11	0.5	0.6	3.33
12	0.5	0.6	3.42
13	0.2	0.425	3.87
14	0.2	0.425	4.35
15	0.2	0.425	3.65
16	0.4	0.425	5.96
17	0.4	0.425	8.54
18	0.4	0.425	4.33
19	0.3	0.3375	3.53
20	0.3	0.3375	4.14
21	0.3	0.3375	4.27
22	0.3	0.3375	0.04

Celal Bayar University Journal of Science
Volume 21, Issue 4, 2025, p 31-42
Doi: 10.18466/cbayarfbe.1597869

23	0.3	0.3375	0.04
24	0.3	0.3375	0.05
25	0.3	0.425	2.73
26	0.3	0.425	5.08
27	0.3	0.425	2.51
28	0.3	0.425	3.73
29	0.3	0.425	2.72

4.2. Validation of the model

In the first step of the statistical analysis, it was recommended to apply a transformation to the data, as the responses range from 0.046 to 8.54, which is a ratio of maximum value to minimum value of the response of 185.57. A wide variation in response values negatively affected the model's accuracy. Accordingly, normal probability distribution graphs obtained as a result of diagnostic analyses of the necessity of transformation were examined in Figure 1. A wide variation in response values negatively affected the model's accuracy. In this case, it was recommended to apply a transformation to the responses. Figure 1a presents results of the non-transformed data, and Figure 1b presents squared root-transformed results. Examination of Figure 1a shows that the normal probability distributions of the residuals deviate from linearity, with clear deviations near the ends of the curved shape. From this point of view, it was seen that the assumption is that the deviation between the actual value and the estimated value, which is defined as the residual, is in accordance with the normal distribution and cannot be fully met. From Figure 1b, it was seen that the residuals are arranged more closely to the linear distribution. After the natural log transformation, it was seen that the deviation in the upper and lower values reduced significantly, and the normal distribution assumption was better provided after the transformation. For this reason, the squared root-transformed model was used in this study.

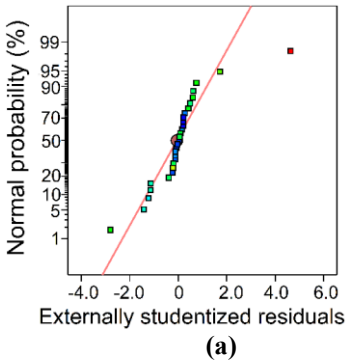

(a)

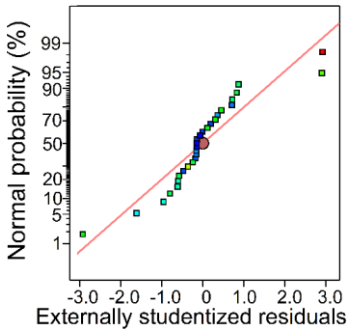

(b)

Figure 1. Diagnostic plots of the model (a) Non-transformed model, (b) Squared root transformed model.

As a result of the statistical analyses, it was determined that the relationship between the independent variables and the response could be described by a quadratic model. ANOVA (Analysis of Variance) was performed to determine the accuracy of the model and ANOVA results are presented in Table 6. It is seen from the table that the R^2 values of the models are very close to 1, which is a desirable situation. Adjusted R^2 and estimated R^2 terms were used to determine the predictive power of the model. Table 6 shows that the adjusted R^2 and estimated R^2 values of the models were relatively high. Since the difference between the adjusted R^2 and the predicted R^2 is less than 0.2, it was understood that the predictions made with the model will give reasonable results. Adequate precision (A.p) measuring a signal-to-noise ratio is greater than 4. The adequate sensitivity value confirmed that the signal-to-noise ratio is acceptable and the model could be used to navigate the design space. The ANOVA results were shown that the p value and F value of the model were less than 0.0001 and 45.32 respectively. F and p values were shown that the model was statistically significant. An F-value of 0.359 for lack of fit meant that the lack of fit was insignificant.

Table 6. ANOVA results

Unconfined compression strength (UCS), Y_1					
Source	**Sum of sq.**	**df**	**Mean sq.**	**F-value**	**p-value**
Model	12.84	7	1.83	45.32	< 0.0001*
X_1	0.3661	1	0.3661	9.05	0.0067**
X_2	4.72	1	4.72	116.65	< 0.0001
$X_1 X_2$	1.06	1	0.398	9.84	0.005
X_1^2	2.73	1	2.73	67.55	< 0.0001
X_2^2	4.82	1	4.82	119.01	< 0.0001
$X_1^2 X_2$	5.72	1	5.72	141.25	< 0.0001
$X_1 X_2^2$	0.2158	1	0.2158	5.33	0.0313
Residual	0.85	21	0.0405		
L. of fit	0.015	1	0.015	0.359	0.558
Pure er.	0.896	20	0.0417		
Cor total	13.69	28			
SD	0.2012	R^2	0.94		
Mean	1.48	Adj.R^2	0.92		
CV(%)	13.63	Pr.R^2	0.89		
		Ap	21.41		

*Significant, **Not significant

As a result of the statistical analysis, a cubic model was developed to predict the UCS depending on the fly ash content and activator amount parameters. The relationship between the predictions provided by the model equations and the UCS of the samples prepared by considering the relevant independent variables was shown in Figure 1. As could be seen in the ANOVA results, there were statistically good match between the predictions of the model and the experimental results (R^2=0.94). In order to verify the obtained model, the USC value was estimated for X_1=0.20 and X_2=0.35 values randomly assigned to the model. Considering X_1 and X_2 values, six samples were prepared and UCS values were determined. Accordingly, model predictions were compared with laboratory test results in Table 7. Accordingly, the model predictions were found to be consistent within the 95% confidence interval.

Table 7. Comparison of the UCS estimation with experimental results.

	Mean (MPa)	95%CI low for mean (MPa)	95%CI high for mean (MPa)
Estimated UCS	4.62	3.83	5.58
UCS test result	5.79	5.09	7.02

4.2. Optimization of independent variables

Response Surface Methodology (RSM) was selected for this optimization study due to its proven efficiency in geotechnical stabilization applications, where it allowed systematic exploration of the experimental domain with minimal experiments while simultaneously optimizing multiple variables (bottom ash content and activator ratio) and their interactions. Central Composite Design (CCD) with $\alpha = 0.5$ was specifically chosen as it requires fewer experimental runs compared to full factorial designs while providing second-order models capable of capturing response surface curvature. The mathematical approach followed a systematic four-step procedure: (1) Data transformation analysis using Box-Cox assessment indicated $\lambda = 0.5$ (square root transformation) to address the wide UCS response range (0.046 to 8.54 MPa, ratio =185.57); (2) improving residual normality and homoscedasticity; Model selection evaluated linear, quadratic, and cubic polynomial models, with the cubic model selected based on highest R^2 value (0.94), significant lack-of-fit test results, and sequential F-test improvements; (3) Parameter estimation employed the least squares method with normal equations $(X'X)\beta = X'Y'$ using Design Expert 12 software algorithms; and (4) Model adequacy checking included residual analysis for normality (Shapiro-Wilk test), independence verification (Durbin-Watson statistic), homoscedasticity testing (Levene's test), and outlier detection using studentized residuals. The final model equation after back-transformation was $UCS = [\beta_0 + \beta_1X_1 + \beta_2X_2 + \beta_{11}X_1^2 + \beta_{22}X_2^2 + \beta_{12}X_1X_2 + \beta_{112}X_1^2X_2 + \beta_{122}X_1X_2^2]^2$ with coefficients $\beta_0 = 1.485$, $\beta_1 = 0.231$, $\beta_2 = 0.829$, $\beta_{11} = -0.631$, $\beta_{22} = -0.839$, $\beta_{12} = 0.394$, $\beta_{112} = -0.913$, $\beta_{122} = -0.177$. Optimization utilized the desirability function method D=(di)^wi with the Modified Feasible Directions algorithm, employing multiple random starting points, gradient vector calculations, and iterative steepest ascent movements within constraints $0.1 \leq X_1 \leq 0.5$ and $0.25 \leq X_2 \leq 0.6$, with convergence criterion $|\nabla D| < 0.001$. Model validation included leave-one-out cross-validation (predicted $R^2 = 0.89$) and independent validation experiments at $X_1 = 0.20$, $X_2 = 0.35$ with six replicate samples, confirming statistical adequacy through t-test comparison ($p > 0.05$), ensuring the optimization results were statistically sound, practically relevant, and reproducible for engineering applications

The combined effect of the activator amount and bottom ash ratio factors on the UCS could be seen from the three-dimensional graphics seen in Figure 2. The optimum area that gives maximum strength could be seen from the contours seen in Figure 2a. As shown in Figures 2a and 2b, the highest UCS values were obtained in the range of X_1 = 0.3-0.5 and X_2 = 0.45-0.5. From Figure 2a, it could be seen that the strength increases due to the increase in the amount of activator in the range of low activator content. Large voids remain in the material due to the consistency-related settlement problem, and at high activator content, the excessive fluidity of the material causes strength losses. The double peaks of the UCS value were seen in Figure 2a and Figure 2b. This situation could be explained by various alkaline activation reactions. Alkali activation was the broadest classification of reactions between the source of alkali metals and silicates. The pH of the grout medium was relatively low and the amount of Ca is relatively high for low X_2 values. Therefore, the system had a high potential to form alkaline active high strength products such as CSH. The second peak (X_2=0.5) could be explained by C(A)SH products. Increasing amount of activator causes high alkalinity. Alumino-silicate gels were often formed in relatively high alkaline environments. The optimization tool in Design Expert 12 statistical software was used to determine the optimum components. In the optimization, some preferences offered by the software for independent variables and responses were used. The "range" preference was used for the independent variables and the "maximum" preference was used for the response. Desirability values (D) between 0 and 1 were taken into account in determining the optimum solutions. Among the ideal values obtained as a result of optimization, X_1=0.49, X_2=0.48 values (D=1) were determined as optimum values. In the study, the optimized ratios were taken into consideration. To better illustrate the optimization process after data transformation, a three-dimensional desirability surface plot (Figure 2b) was generated based on the square root-

Celal Bayar University Journal of Science
Volume 21, Issue 4, 2025, p 31-42
Doi: 10.18466/cbayarfbe.1597869

transformed UCS values. The transformation was applied to reduce the variability of the response and ensure a more statistically robust model, as indicated by the diagnostic residual plots and improved normality. Following the transformation, the UCS values were normalized to a [0–1] scale to compute desirability scores, where 1 represents the most desirable outcome. Using these normalized values, a cubic interpolation was applied over the experimental domain defined by the bottom ash-to-soil ratio (X_1) and the activator-to-dry matter ratio (X_2). The resulting surface reveals a well-defined optimum region, with the peak desirability ($D \approx 1$) located around $X_1 \approx 0.49$ and $X_2 \approx 0.48$. This graphical representation confirmed that the optimized mix design achieved a global optimum, and the transformation-enhanced model supported accurate prediction and decision-making

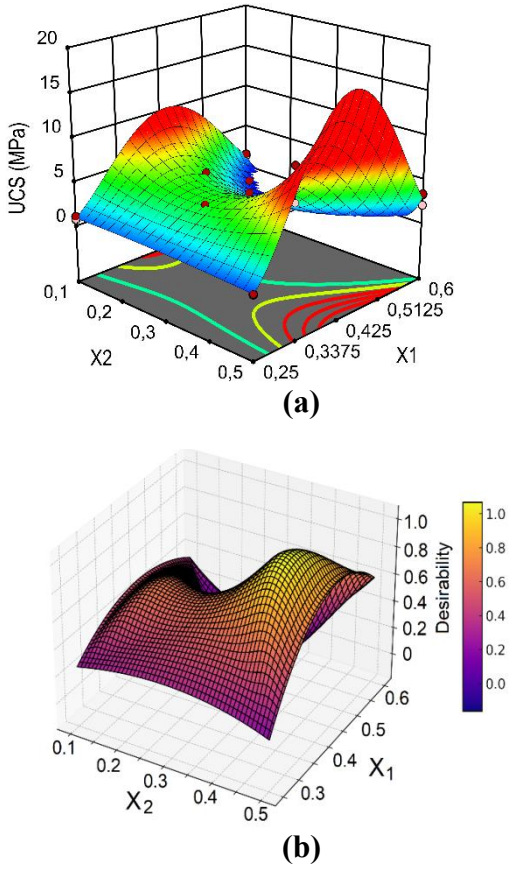

Figure 2. 3D plots **(a)** presents interaction between activator content and AAB content, **(b)** showing the optimum desirability surface.

Table 8 presented the optimization results obtained through the desirability function approach. The table included the key input parameters, bottom ash to soil ratio (X_1) and activator to dry matter ratio (X_2), along with the UCS values and their corresponding desirability scores. A desirability score of 1.000 indicated the most favorable combination for strength development. This tabular format enhanced the interpretability of the optimization process by providing a concise summary of the optimal mix designs.

Table 8. Optimization results

	X_1 Range 0.1-0.5	X_2 Range 0.25-0.6	Pred. UCS (MPa) Maximized	Desirability
1	0.49	0.48	5.93	1
2	0.45	0.50	5.80	0.964
3	0.50	0.47	5.71	0.951
4	0.42	0.43	5.55	0.922

5. Carbon footprint analyses

In this section, the analysis focused on estimating the potential carbon emissions resulting from the production of DSM columns. The assessment was based on a grout formulation composed of sodium silicate, sodium hydroxide, fly ash, waste tuff, and additional sodium hydroxide, using the optimal mix proportions identified in the current study. Figure 3 presented an overview of the emission calculation workflow. Specifically, the CO_2 emissions associated with the manufacturing and transportation of both the chemical activators and binders, as well as the grout preparation and the actual implementation of DSM columns, were quantified separately.

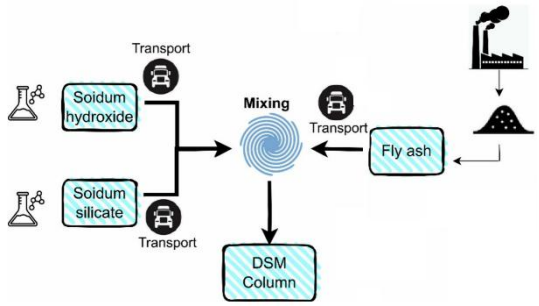

Figure 3. Schematic diagram of the DSM column production process.

Table 9 presented the carbon emission factors associated with the materials utilized in the soil stabilization process. In accordance with recent updates in European legislation, fly ash was no longer categorized as waste but rather as a by-product. Consequently, its carbon emission factor was adopted as 2.280×10^{-2} $kgCO_2/m^3$ [32]. The emission data listed in the table for sodium silicate refer specifically to its solid-state form. As noted by Davidovits [33] when sodium silicate was used in solution form (Na_2SiO_3), the CO_2 emissions could be reduced by up to 55%. Based on this, the adjusted carbon emission factor for sodium silicate solution was calculated as $0.45\times 1.248 = 0.5616$ $kgCO_2/kg$ [34]. In addition, a 10 M sodium hydroxide (NaOH) solution was considered when estimating the activator-related emissions, with its emission factor taken as 0.4173 $kgCO_2/kg$.

Table 9. Carbon emission factors taken into account for carbon foot print calculations of raw materials [31].

Material	Unit	Carbon emission factor
Fly ash	kg CO_2/kg	2.7×10^{-2}
Na_2SiO_3 (Solid)	kg CO_2/kg	1.248
NaOH (Solid)	kg CO_2/kg	1.448
OPC	kg CO_2/kg	0.81

Table 10 outlined the assumed transport distances and corresponding emission factors relevant to the delivery of stabilization materials. Additionally, the estimated carbon emissions generated by the operation of deep mixing equipment, which included a 280 hp excavator, a 130 hp mobile silo unit with a single tank, a 60 hp compactor, and a mixing attachment. According to the TS EN 14679 standard, the production rate of a DSM column ranged between 0.08 m³ and 0.25 m³ per minute. The fuel consumption for the entire equipment system was assumed to be approximately 40.185 kg (or 47.23 liters) of diesel per hour. Based on these values, the CO_2 emission factor associated with producing 1 m³ of DSM column was calculated as 11.83 kg CO_2/m³ (source: https://www.komatsu.eu/en/hybrid/carbon-footprint-calculator).

Table 10. Carbon emission factors of transportation [31].

Material	Means of transport	Distance	Emission factor
Fly ash	Medium diesel truck (8 t)	300 km	0.149 kg CO_2/tkm
Na_2SiO_3	Light diesel truck (2 t)	60 km	0.212 kg CO_2/tkm
NaOH	Light diesel truck (2 t)	60 km	0.212 kg CO_2/tkm

Table 11 summarized the carbon emissions associated with the application of 1 m³ DSM columns. The calculations were based on the optimal material proportions required to produce 1 m³ of grout with a unit weight of 18.3 kN/m³, as determined in the study. The minimum UCS value recommended by FHWA for deep mixing columns was 2 MPa. As a result of the control tests, it was determined that X_1=0.25 and X_2=0.35 values gaved UCS (5.79 MPa) above the lower limit value of 2MPa, so these values were taken into consideration in the calculations. Emission estimation was conducted in three stages: (i) CO_2 emissions from the manufacturing of constituent materials, (ii) emissions generated during their transportation to the construction site, and (iii) emissions resulting from the operation of deep mixing machinery. Additionally, Table 11 provided a comparative evaluation of the total CO_2 output from alkali-activated DSM columns and conventional soil–cement columns, with both comparisons standardized per cubic meter of column volume. For the soil–cement alternative, a cement dosage ranging between 160–440 kg/m³ was reported in the literature [35] and 300 kg/m³, 400kg/m³ were adopted for the current analysis. The water-to-cement ratio used in grout preparation was taken as 1.25. According to the findings, producing 1 m³ of OPC-based DSM column results in approximately 258.99 kg of CO_2 emissions, whereas the same volume of alkali-activated DSM column emited around 242.57 kg of CO_2.

6. The effect of polypropylene fiber content on UCS

Although the present study utilized 6 mm long polypropylene fibers based on nozzle-size constraint and compatibility with deep mixing equipment, fiber length played a critical role in stress transfer efficiency and crack-bridging capacity. Longer fibers may improve energy absorption but can also lead to entanglement and poor dispersion, especially in high-fluidity slurries. The 6 mm fiber length ensured adequate dispersion within the matrix, as visually confirmed during mixing. However, future studies should explore different fiber lengths and use image-based or statistical methods to quantify dispersion effects on UCS and ductility.

In order to determine the optimum polypropylene fiber ratios of the mixtures for which the optimum fly ash and activator ratios were determined by the response surface method, soil samples were prepared in accordance with the sample preparation method recommended by the US Highway Administration (FHWA) for deep mixing columns. The test specimens were cylindrical specimens with a height of 100 mm and a diameter of 50 mm. The specimens were cured in an oven at 28 °C for 7 days. The effect of fiber content on UCS, strain at failure, and modulus of elasticity properties of 7-day cured samples was presented in Fig.4a, 4b, and 4c, respectively. In Fig.4a, it was seen that the best UCS values were obtained from the samples stabilized with 1.50%, and 1.75% fiber contents. Polypropylene fiber showed positive effects on soil stabilization. However, fiber amounts above a certain fiber content (1.50%) led to a decrease in UCS value. A similar trend to Fig. 4a was

Table 11. Carbon emissions calculated for 1 m³ alkali activated, and OPC added DSM columns

	NaOH	Na_2SiO_3	FA	Soil	OPC	Water
Amounts for 1 m³ DSM column (kg)	237.22	237.22	225.9	1129.63	300	375
CO_2 release during production (kgCO_2)	98.99	133.22	6.1	-	243	-
CO_2 release during transportation (kgCO_2)	1.508	1.508	1.26	-	1.676	2.385
CO_2 release during DSM column production (kgCO_2)			11.83			
Total CO_2 release for alkali activated 1 m³ DSM column (kgCO_2)			242.57			
Total CO_2 release for OPC added 1 m³ DSM column (kgCO_2)			258.99			

seen in Fig. 4b. As expected, with increasing fiber content, the strain value at failure increased, in other words, the material ductility increased (Fig.4b). Fiber contents of 1.5% and 1.75% significantly increased the ductility of the material. Fiber amounts higher than this fiber content (1.5% and 1.75%) caused the ductility to decrease. It was clear that fiber additive increased the UCS values of stabilized samples. However, varying fiber contents caused a limited increase in UCS (Fig.4a). Figure 4c showed that the modulus of elasticity was higher for relatively low fiber contents. This could be explained by low strain at the failure value of the relatively low fiber contents with respect to relatively high fiber contents.

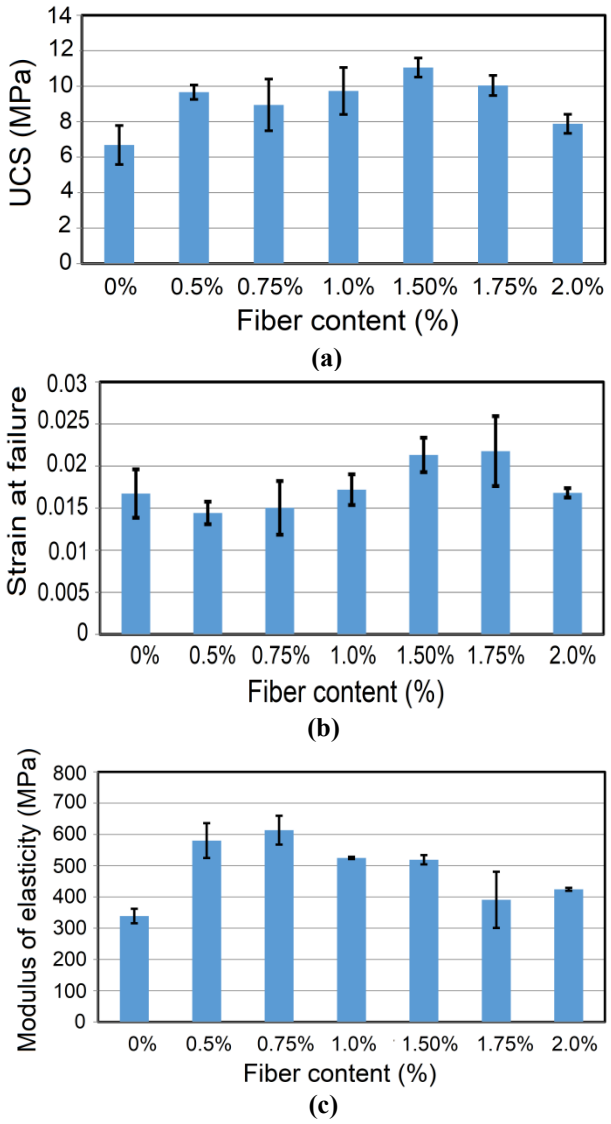

Figure 4. The effect of fiber content on **(a)** UCS, **(b)** Strain at failure, **(c)** Modulus of elasticity

7. The effect of curing temperature on the stabilized samples

Fig.5 presented the effect of curing temperature on some mechanical properties of stabilized soil. In this context, soil samples were prepared by considering the amounts of fiber, activator, and binder giving maximum strength. The prepared samples were subjected to curing for 7 days at ambient temperatures of 5 °C, 10 °C, 20 °C and 30 °C. The curing temperatures selected in this study simulate possible subsurface thermal conditions experienced by deep mixing columns at various soil depths. For example, in regions with annual surface temperatures ranging from 5–15 °C, soil temperatures at depths of 3–10 meters often stabilized around 10–20 °C, depending on soil type and geothermal gradient. The 30°C condition represented shallow depths in warm climates or thermally active regions. These curing conditions were thus representative of practical field scenarios and support the generalizability of the experimental results. UCS tests were performed on the samples and the effects of curing temperature on the UCS and modulus of elasticity of the samples were investigated.

The effect of curing temperature on UCS values of the samples was presented in Fig.5a. The figure showed a gradual increase in UCS values with the increase in curing temperature in the specimens. The highest UCS value was observed in samples cured at 30 °C, while at 20 °C, cured samples have 1.5 times less UCS than soil specimens cured at 30 °C. Fig.5b presents relations between curing temperature and modulus of elasticity. It was seen from the figure that the modulus of elasticity values at curing temperatures of 20 °C and 30 °C were close to each other, but the modulus of elasticity values of the samples cured at 30 °C gives the highest value.

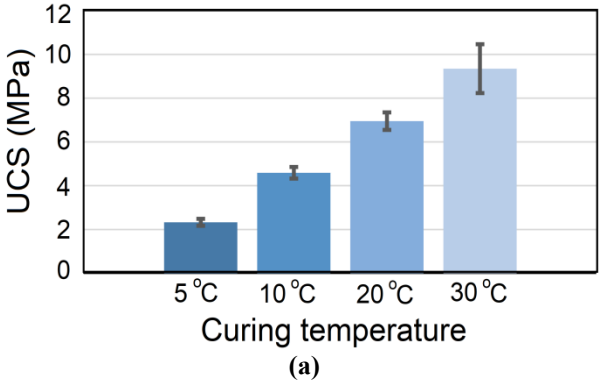

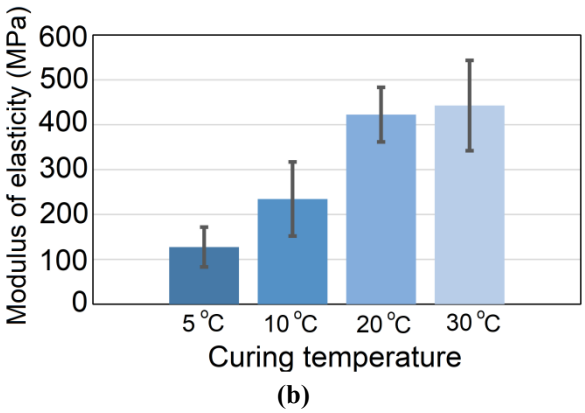

(b)

Figure 5. The effect of curing temperature on **(a)** UCS, **(b)** Modulus of elasticity of the samples.

8. Conclusions

This study focused on the optimization of alkali-activated bottom ash and polypropylene fiber content in deep mixing column mortar for soil stabilization applications. RSM was employed to optimize the precursor and activator amounts, and the statistical model exhibited high predictive accuracy for UCS values of the stabilized soil.

The results indicated that the highest UCS values were achieved with alkali-activated bottom ash and activator content in the range of 0.3-0.5 and 0.45-0.5, respectively. Polypropylene fiber was found to positively impact soil stabilization, with optimal UCS values observed at fiber contents of 1.50% and 1.75%. However, excessive fiber content led to a decrease in UCS.

By addressing three interrelated factors—material optimization, mechanical enhancement via fiber, and environmental curing conditions—this study presented a holistic approach to DMC performance improvement. Mechanical properties of soil increased remarkably with varying curing temperature. Considering that the soil temperature varied depending on various parameters throughout the soil depth, it is seen that the mechanical properties of deep mixing columns would be different throughout the soil depths. The bearing capacity of the deep mixing columns was likely to vary due to the variation in curing temperature.

In addition to mechanical performance, the study evaluated the environmental impact of alkali-activated DMC mixtures through a carbon footprint analysis. Results indicated that the optimized alkali-activated mixture lead to a lower CO_2 emission (242.57 kg CO_2/m^3) compared to the conventional OPC-based mixture (258.99 kg CO_2/m^3). This reduction, combined with the utilization of industrial by-products, highlights the ecological advantage of the proposed binder system, supporting the development of more sustainable geotechnical engineering practices.

The findings highlighted the importance of optimizing the composition of alkali-activated materials and considering the addition of reinforcing fibers for effective soil stabilization. Additionally, the consideration of curing temperature effects on the mechanical properties of deep-mixed columns emphasized the need for a comprehensive understanding of environmental factors in soil stabilization practices.

In summary, the combination of alkali-activated bottom ash, polypropylene fiber, and careful consideration of curing conditions presents a promising approach for enhancing the mechanical properties and durability of deep mixing column mortar in soil stabilization applications. Although a detailed cost analysis was not within the scope of this study, the optimized mixture developed herein provides a promising alternative for practical deep mixing column applications due to its enhanced strength, ductility, carbon footprint. The use of industrial by-products such as bottom ash supports sustainable engineering practices and may contribute to reducing the environmental impact of ground improvement. Future studies will include environmental and economic evaluations to establish the feasibility of large-scale implementation.

Author's Contributions

Fatih Yılmaz: Supervised experimental process. Helped in manuscript preparation.

Büşra Avlayan: Assisted and conducted experimental process.

Hakan Alper Kamiloğlu: Drafted and wrote the manuscript, performed statistical analyses. Supervised result interpretation.

Ethics

There are no ethical issues after the publication of this manuscript.

References

[1]. Kitazume M, Terashi M. The Deep Mixing Method; CRS Press: Taylor & Francis Group, Tokio, Japan; 2013.

[2]. Ekmen AB, Algın HM , Özen M. 2020. Strength and stiffness optimisation of fly ash-admixed DCM columns constructed in clayey silty sand. *Transportation Geotechnics;* 24 : 100364, https://doi.org/10.1016/j.trgeo.2020.100364.

[3]. Yang S, Zhang D, Tamura S, Hongjiang L, Anhui W. 2025. Investigation of seismic performance of group piles with different cement soil improvements in liquefiable sands: shaking table test. *International Journal of Civil Engineering* https://doi.org/10.1007/s40999-025-01121-0

[4]. Amer AA, El-Hoseny S. 2017. Properties and performance of metakaolin pozzolanic cement pastes. *Journal of Thermal Analysis and Calorimetry*;129 : 33–44. https://doi.org/10.1007/s10973-017-6087-9.

[5]. Öksüzer N. 2023. The effect of calcination on alkali-activated lightweight geopolymers produced with volcanic tuffs. *Journal of the Australian Ceramic Society*; 59:1053-1063 https://doi.org/10.1007/s41779-023-00896-6.

[6]. Yılmaz F, Kuvat A, Kamiloğlu HA. 2023. Optimizing and investigating durability performance of sandy soils stabilized with alkali activated waste tuff-fly ash mixtures. *Sādhanā*; 48:185. https://doi.org/10.1007/s12046-023-02250-9.

[7]. Kumar A, Saravanan TJ, Bisht K, Kabeer K. 2021. A review on the utilization of red mud for the production of geopolymer and alkali activated concrete. *Construction and Building Materials*; 302, 124170. https://doi.org/10.1016/j.conbuildmat.2021.124170.

[8]. Alves BIA, Marvila MT, Linhares Júnior JAT, Vieira CMF, Alexandre J, de Azevedo ARG. 2024. Alkaline activation of binders: a comparative study. *Materials (Basel)*;17 : 667. https://doi.org/10.3390/ma17030667.

[9]. Nouhi S, Khaksar Najafi E, Zanganeh Ranjbar P, Payan M, Jamshidi Chenari R. 2024. Geotechnical performance of alkali-activated uncalcined clayey soils with hydroxide and aluminate-based activators. *Journal of Materials in Civil Engineering*;36. https://doi.org/10.1061/JMCEE7.MTENG-16746.

[10]. Hamid Abed M, Hamid Abed F, Alireza Zareei S, Sabbar Abbas I, Canakci H, Kurdi NH, et al 2024. Experimental feasibility study of using eco- and user-friendly mechanochemically activated slag/fly ash geopolymer for soil stabilization. *Clean Mater*;11:100226. https://doi.org/10.1016/j.clema.2024.100226.

[11]. Martins Lima B, Bruschi GJ, Festugato L, Consoli NC. 2024. Mechanical behavior of a granular soil stabilized with alkali-activated waste. *Journal of Materials in Civil Engineering*; 36. https://doi.org/10.1061/JMCEE7.MTENG-15641.

[12]. Komaei A, Saeedi A. 2025. Pumicite-based geopolymer optimization for sustainable soil stabilization. *Journal of Materials in Civil Engineering*, 37:6, 04025141. https://doi.org/10.1061/JMCEE7.MTENG-19308.

[13]. Hamed E, Demiröz A. 2024. Optimization of geotechnical characteristics of clayey soils using fly ash and granulated blast furnace slag-based geopolymer. *Construction and Building Materials* ;441:137488. https://doi.org/10.1016/j.conbuildmat.2024.137488.

[**14].** Juengsuwattananon K, Winnefeld F, Chindaprasirt P, Pimraksa K. 2019. Correlation between initial SiO_2/Al_2O_3, Na_2O/Al_2O_3, Na_2O/SiO_2 and H_2O/Na_2O ratios on phase and microstructure of reaction products of metakaolin-rice husk ash geopolymer. *Construction and Building Materials*;226:406–17. https://doi.org/10.1016/j.conbuildmat.2019.07.146.

[15]. Kamiloğlu HA, Kurucu K, Akbaş D. 2024. Investigating the effect of polypropylene fiber on mechanical features of a geopolymer-stabilized silty soil. *KSCE Journal of Civil Engineering*;28:628–43. https://doi.org/10.1007/s12205-023-0488-z.

[16]. Shu Y, Song Y, Fan, H, Wang D, Lu , Huang Y, Zhao C, Chen L, Song, X. 2024. Fiber-reinforced microbially induced carbonate precipitation (MICP) for enhancing soil stability: mechanisms, effects, and future prospects. *Journal of Building Engineering*; 94:109955. https://doi.org/10.1016/j.jobe.2024.109955

[17]. Al-Dossary AAS, Awed AM, Gabr AR, Fattah MY, El-Badawy SM. 2023. Performance enhancement of road base material using calcium carbide residue and sulfonic acid dilution as a geopolymer stabilizer. *Construction and Building Materials*; 364:129959. https://doi.org/10.1016/j.conbuildmat.2022.129959.

[18]. Harmal A, Khouchani O, El-Korchi T, Tao M, Walker HW. 2023. Bioinspired brick-and-mortar geopolymer composites with ultra-high toughness. *Cement and Concrete Composites*;137:104944. https://doi.org/10.1016/j.cemconcomp.2023.104944.

[19]. Sukontasukkul P, Jamsawang P. 2012. Use of steel and polypropylene fibers to improve flexural performance of deep soil–cement column. *Construction and Building Materials*; 29:201–205. https://doi.org/10.1016/j.conbuildmat.2011.10.040.

[20]. Ekmen AB, Algın HM. 2023. Optimization of fiber-reinforced deep cement-fly ash mixing column materials. *Revista de la Construcción. Journal of Construction;* 22:3:707-728. https://doi.org/10.7764/RDLC.22.3.707.

[21]. Avcı Y, Ekmen AB. 2023. Artificial intelligence assisted optimization of rammed aggregate pier supported raft foundation systems based on parametric three-dimensional finite element analysis. *Structures;* 56:105031. https://doi.org/10.1016/j.istruc.2023.105031.

[22]. Zangeneh N, Azizian A, Lye L, Popescu R. Application of response surface methodology in numerical geotechnical analysis. 55th Can. Soc. Geotech. Conf., Hamilton, Ontario, Canada: 2002.

[23]. Deshpande TD, Kumar S, Begum G, Basha SAK, Rao BH. 2021. Analysis of railway embankment supported with geosynthetic-encased stone columns in soft clays: a case study. *International Journal of Geosynthetics and Ground Engineering*; 7:43. https://doi.org/10.1007/s40891-021-00288-5.

[24]. Yao K, Yao Z, Song X, Zhang X, Hu J, Pan X. 2016. Settlement evaluation of soft ground reinforced by deep mixed columns. *International Journal of Pavement Research and Technology*;9:460–5. https://doi.org/10.1016/j.ijprt.2016.07.003.

[25]. Phutthananon C, Jongpradist P, Wonglert A, Kandavorawong K, Sanboonsiri S, Jamsawang P. 2023. Field and 3D numerical ınvestigations of the performances of stiffened deep cement mixing column-supported embankments built on soft soil. *Arabian Journal for Science and Engineering*; 48:5139–69. https://doi.org/10.1007/s13369-022-07322-2.

[26]. Voottipruex P, Bergado DT, Suksawat T, Jamsawang P, Cheang W. 2011. Behavior and simulation of deep cement mixing (DCM) and stiffened deep cement mixing (SDCM) piles under full scale loading. *Soils and Foundations*; 51 : 307–320. https://doi.org/10.3208/sandf.51.307.

[27]. Chen S, Guan Y, Dai J, Zhao W. 2023. Field experimental and numerical studies on performance of concrete–cored gravel column-supported embankments. *International Journal of Geomechanics*; 23. https://doi.org/10.1061/IJGNAI.GMENG-8263.

[28]. Bhavita Chowdary V, Ramanamurty V, Pillai RJ. 2021. Experimental evaluation of strength and durability characteristics of geopolymer stabilised soft soil for deep mixing applications. *Innovative Infrastructure Solutions*; 6:40. https://doi.org/10.1007/s41062-020-00407-7.

[29]. Jastrzębska M. 2025. Use of alternative materials in sustainable geotechnics: state of world knowledge and some examples from Poland. *Applied Sciences,* 15, 6: 3352. https://doi.org/10.3390/app15063352.

[30]. Sabziparvar A, Khoshhal Jahromi F. 2022. Evaluating the most effective climatic parameters affecting the monthly mean soil temperature estimates using the PLS method. *Arabian Journal of Geosciences*;15:1044. https://doi.org/10.1007/s12517-022-10297-x.

[31]. Bruce M, Berg R, Collin J, Filz G, Terashi M, Yang DS. Federal Highway Administration design manual: Deep mixing for embankment and foundation support. United States Federal Highway Administration Offices of Research & Development 2013.

[32]. Shi X, Zhang C, Liang Y, Luo J, Wang X, Feng Y, Li Y, Wang Q Consistency Abomohra AE-F. Life cycle assessment and impact correlation analysis of fy ash geopolymer concrete. *Materials (Basel)*, 14(23):7375 2021.

[33]. Davidovits J. False values on CO2 emission for geopolymer cement/concrete published in scientific papers. Geopolymer Institute. Library.https://www.geopolymer.org/library/technicalpapers/falseCO_2-values-published-inscientific-papers/. Accessed 15 May 2024

[34]. Setiawan AA, Hardjasaputra H, Soegiarso R. 2023. Embodied carbon dioxide of fy ash based geopolymer concrete. *e. IOP Conf Ser Earth. Environ. Sci,* 1195(1):012, 1. https://doi.org/10.1088/1755-1315/1195/1/012031

[35]. Farouk A, Shahien MM. 2013. Ground improvement using soil–cement columns: experimental investigation . *Alexandria Engineering Jpurnal. 52(4):733–740. https://doi.org/10.1016/j.aej.2013.08.009*